

Superhydrophobic Lignocellulosic Wood Fiber/Mineral Networks

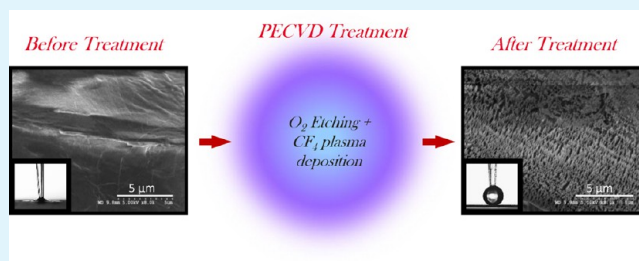
Mehr Negar Mirvakili, Savvas G. Hatzikiriakos, and Peter Englezos*

Department of Chemical and Biological Engineering and Pulp and Paper Centre, The University of British Columbia, 2360 East Mall, Vancouver, BC V6T 1Z3, Canada

S Supporting Information

ABSTRACT: Lignocellulosic wood fibers and mineral fillers (calcium carbonate, talc, or clay) were used to prepare paper samples (handsheets), which were then subjected to a fluorocarbon plasma treatment. The plasma treatment was performed in two steps: first using oxygen plasma to create nanoscale roughness on the surface of the handsheet, and second fluorocarbon deposition plasma to add a layer of low surface energy material. The wetting behavior of the resulting fiber/mineral network (handsheet) was determined. It was found the samples that were subjected to oxygen plasma etching prior to fluorocarbon deposition exhibit superhydrophobicity with low contact angle hysteresis. On the other hand, those that were only treated by fluorocarbon plasma resulted in “sticky” hydrophobicity behavior. Moreover, as the mineral content in the handsheet increases, the hydrophobicity after plasma treatment decreases. Finally, it was found that although the plasma-treated handsheets show excellent water repellency they are not good water vapor barriers.

KEYWORDS: superhydrophobic, paper, plasma, PECVD, filler, cellulose



1. INTRODUCTION

Changing the wetting behavior of a surface to render it superhydrophobic may facilitate the development of novel materials in a wide range of potential applications.^{1,2} The wettability of a surface is typically quantified in terms of the static and the dynamic contact angles (advancing and receding) with a water droplet. Superhydrophobic surfaces, which refer to surfaces with a water contact angle above 150° and contact angle hysteresis of less than 10°, have recently received tremendous attention in the literature due to their proven significance in industrial applications.² It is well established and understood that a combination of low surface energy and roughness are the main ingredients for the fabrication of hydrophobic surfaces. In most cases both surface chemistry and surface roughness should be modified to create a superhydrophobic substrate, also known as lotus effect, which makes the process challenging.^{3,4} Interestingly, most of the fabricated superhydrophobic surfaces are not from renewable and biodegradable materials.⁵ On the other hand, the cellulosic surface made with wood and/or nonwood plant fibers provides a suitable platform. By rendering the cellulosic surface hydrophobic, a number of value-added applications can be pursued based on this biodegradable, renewable, and thus sustainable biopolymer which is abundant in nature.

Paper has a hydrophilic surface because the cellulosic fibers contain hydrophilic groups such as hydroxyl and carboxyl groups. This inherent hydrophilicity poses some limitations in the applications, where hydrophobicity is highly required. For example, in packaging applications water and moisture resistance is a required property.⁶ It is customary to improve the water resistance by employing internal sizing, surface sizing,

and conventional barrier coating layers.⁷ There is a limitation, however, due to the high cost of thick coating layers and the poor recyclability of the sized paper.

Fluorocarbon thin-film coatings by plasma-enhanced chemical vapor deposition (PECVD) present several advantages over the conventional coating methods. The amount of fluorocarbons that is deposited on the surface of paper can be controlled depending on the degree of water repellency that is required. The fluorocarbon films that are deposited by PECVD are thin and breathable, and thus the paper is not as difficult to recycle as the coated papers with thick layers of coating by conventional methods.⁸ Also a single thin film of deposited fluorocarbon on the surface of paper eliminates the need for multiple layer coatings to achieve barrier properties.

The first application of plasma treatment on a cellulosic surface was performed in the 1970s by using microwave plasma for the modification of the bonding properties of cellulose.^{9–12} A variety of precursor gases such as N₂, Ar, O₂, H₂, NH₃, SO₂, hydrocarbons, fluorocarbons, halogens, and organosilanes have been used depending on the desired properties of the cellulosic surface.¹¹ Pure cellulose is hydrophilic with a water contact angle of around 20°. However, depending on the pulping technique, the wood fiber may contain different amounts of cellulose, lignin, hemicelluloses, and extractives, and this will affect the final wettability of the handsheet.

Hydrocarbon, organosilicon, and fluorocarbon plasma treatment have been employed to make hydrophobic paper

Received: June 12, 2013

Accepted: August 19, 2013

Published: August 19, 2013

Table 1. Composition of Pulp Suspension²¹

1.02%		4.28%		0.167%		0.011%		0.006%	
filler (%)	V (mL)	pulp (g)	water (g)	starch (kg/t)	V (mL)	floc. (kg/t)	V (mL)	silica (kg/t)	V (mL)
25	8.6	6.1	485	10	2.1	0.3	1.0	0.4	2.3
35	12.0	5.3	483	10	2.1	0.3	1.0	0.4	2.3
45	15.4	4.5	480	10	2.1	0.3	1.0	0.4	2.3

surfaces.¹³ One of the desired properties of plasma deposition is the individual coverage of fibers by polymer thin film which does not block the interfiber pores.¹¹ The effect of cold (O_2 and H_2) plasma treatment on two cellulose materials (filter paper from pure cotton cellulose, a greaseproof paper made from sulfite pulp fibers) was investigated by Carlsson and Strom.¹⁴ They reported reduction of hydroxyl groups and creation of low molecular weight material on cellulose after H_2 plasma and oxidation and reduction of the surface after O_2 plasma. The increase in hydrophilicity and water absorption was reported after oxygen plasma processing and was attributed to the oxidation of lignin and extractives of the fiber.¹⁵ The first fluorocarbon treatment of paper from kraft pulp was reported by Sapiuha et al.^{16,17} Different ratios of CF_4 and O_2 were tested, and it was found that by increasing the CF_4 flow rate the water absorption time increases.

It is known that the surface of paper on the felt side differs in terms of roughness and chemical concentration from that on the wire side. This characteristic, referred to as “two-sidedness”, was studied by Sahin et al.¹⁸ by deposition of CF_4 film on paper from kraft fibers and free of any additives. They reported that the felt side is more prone to fluorination than the wire side due to the concentration of coarse fibrous materials on the felt side. Finally, Vaswani et al.⁸ reported using pentafluoroethane (CF_3CHF_2) and octafluorocyclobutane (C_4F_8) to create a hydrophobic paper. The water vapor diffusion through this paper was found to occur readily.

The atmospheric nonthermal plasma processing provides some advantages over the typical surface modification methods to create superhydrophobic paper. It is a solvent-free method. The waste and byproduct generation is very low, and the energy-intensive drying process is not required. Finally, plasma surface modification is an effective way of controlling the surface energy and chemical properties of substrates without affecting their bulk ones.¹³

This study presents the results of the effect of O_2 etching and CF_4 plasma deposition on the wetting behavior of the surface of handsheets made with thermomechanical wood fibers and filled with three types of fillers (precipitated calcium carbonate, kaolin clay, and talc) at three levels of concentration. In addition, the effect of fiber length on the wetting behavior is determined. The effect of plasma treatment on paper properties, such as tensile strength, and water absorption are also discussed.

2. EXPERIMENTAL DETAILS

2.1. Paper Sample (Handsheet) Preparation. All handsheets were prepared using a modified handsheet former on an applied vacuum.¹⁹ The former is constructed of two 3" diameter clear acrylic circular cylinders which are located above and below the forming fabric. A flush mounted pressure transducer (GP: 50 model 218-C-SZ-10-SG) is located in the wall of the test chamber below the forming fabric. A vacuum chamber which is made of a 13 mm thick PVC sheet is connected to the bottom of the test chamber by a 20 mm diameter

PVC pipe and electrically actuated solenoid valve. All handsheets were made at the vacuum pressure of -34 KPa (10 inHg). The selection of suction pressure is based on the pressure range that is encountered in industrial processes.²⁰

The peroxide-bleached TMP (thermo mechanical pulp) had a pH of 6.9 ± 0.2 and consistency of 4.3% supplied by Catalyst Paper, and it was a mixture of spruce, fir, and pine fibers. The handsheets were prepared using three different fillers, namely, precipitated calcium carbonate, kaolin clay (39% Al_2O_3 , 46% SiO_2 , 13% H_2O), and talc (63% SiO_2 , 32% MgO , 5% H_2O). The PCC (precipitated calcium carbonate) filler was obtained from Specialty Minerals Inc. (Bethlehem, Pennsylvania, USA) with the particle shape of rosette, average particle size of $10.2 \mu m$ (measured by Scircco 2000 Mastersizer, the provider technical data sheet reported the median particle size of $1.3 \mu m$), dry brightness of 98%, and a zeta potential value of -17.8 ± 0.3 mV (measured by Zetasizer 2000) at a concentration of 0.002 wt % in water. The kaolin clay filler was obtained from the Pulp and Paper Center in UBC and has an average particle size of $13.5 \mu m$ and a zeta potential value of -15.1 ± 0.7 mV at a concentration of 0.002 wt % in water. Also, the talc filler had an average particle size of $34.7 \mu m$ and zeta potential value of -12.5 ± 2.5 mV at a concentration of 0.002 wt % in water. The chemicals used in the preparation of handsheets were cationic tapioca starch (S880, National Starch ULC, Surrey, BC, Canada) with the N content of 0.9–1.10% and an average molecular weight of 3×10^6 g/mol, cationic flocculent (acrylamide copolymer) supplied by Eka Chemicals (Magog, QC, Canada) with the average molecular weight of 10×10^6 g/mol, silica as a 8.1 wt % suspension supplied by Eka Chemicals (Magog, QC, Canada) with the mean size of 5 nm, and water used for the preparation of filler and polymer solutions.

A suspension of 1.7 wt % starch was prepared according to the procedure provided by National Starch ULC.²¹ The pulp suspension was prepared with concentrations shown in Table 1. The formed handsheets were dried and kept in the condition room prior to surface treatment.

Fiber Classification. One set of experiments was performed by making handsheets with three different size fiber lengths. The pulp was classified into five different fiber lengths using the Bauer–McNett classifier according to TAPPI standard T233 cm-95. The fibers were collected from the screen openings of 1.19, 0.595, 0.297, 0.149, and 0.074 mm. The Tyler series numbers for these openings are 14, 28, 48, 100, and 200. The length of the classified fibers from openings of 48, 100, and 200 were measured by HiRes Fiber Quality Analyzer (OpTest Equipment Inc.). Different handsheets were prepared by mixing 50% of the unclassified pulp with 50% of the classified pulp from openings 48, 100, and 200 with mean fiber length of 1.5, 0.70, and 0.36 mm, respectively. Therefore, three different handsheets were prepared in which the dominant fiber length was 1.5, 0.70, and 0.36 mm.

2.2. Surface Plasma Treatment. The plasma treatment of the samples was performed using Trion/RIE (reactive ion etch) plasma-enhanced chemical vapor deposition (PECVD) (model: ACD) with a vacuum loadlock, 250 V AC, and a frequency of 60 Hz.²²

Handsheets Treatment. The oxygen plasma for etching the handsheets and CF_4 plasma for thin-film deposition were used. The PECVD operation parameters are summarized in Table 2.

The handsheets were treated at two different etching times of 15 and 20 min at an O_2 flow rate of $10 \text{ cm}^3/\text{min}$. The CF_4 deposition was performed for 20 min at three levels of flow rates, 40, 30, and $10 \text{ cm}^3/\text{min}$.

Table 2. PECVD Operation Parameters

precursor gas	pressure (mTorr)	power (W)	T (°C)
O ₂	100	300	20
CF ₄	1000	200	20

2.3. Contact Angle Measurements. The contact angle of water droplets was measured by the goniometry method by capturing images with a high-resolution camera under a light source. A 2 μ L water droplet (resistivity of 18.2 M Ω cm at 25 °C, a total organic C content <10 ppb, pH 7) was dispensed on the respective surfaces with a piston-driven air displacement pipet. Digital images of the water droplet on the surfaces were taken with a Nikon D90 digital camera. The contact angles were determined by analyzing droplet images with the software FTA32 Version 2.0. Advancing and receding contact angles were determined by the “add and remove” volume method. The camera was set to capture three images per second for advancing and receding contact angle analysis.

2.4. Surface Analysis. Scanning Electron Microscopy (SEM). The surface structures of the handsheets before and after plasma etching and deposition were analyzed with a Hitachi S-3000N-VP SEM at operating voltage of 5–10 kV. The variable-pressure mode was selected since the paper and the CF₄ films are insulators. The EDX (energy-dispersive X-ray spectroscopy) analysis of handsheets in Z-direction was performed using the SEM. Three areas over the handsheet surface were selected for analysis (Supporting Information Figure S1 (a)). The top side and the wire side of the handsheets were analyzed. Also, the sheets were divided into four areas, and each area was analyzed for mineral content (Supporting Information Figure S1 (b)).

X-ray Photoelectron Spectroscopy (XPS). XPS was used to determine the elemental composition of the material surface. This technique is capable of scanning the first 10 nm of the surface. The spectra were collected using the Omnicron & Leybold model MAX200 XPS with Al K- α X-rays and 15 kV, 20MA emission current.

FTIR-ATR. Fourier transform infrared spectra (FTIR) with attenuated total reflectance (ATR) were obtained with a Thermo Nicolet AVATAAR 360 FTIR spectrometer. The samples were cut (0.5 \times 0.5 cm) and pressed against the ATR crystal using a flat metal with a controlled pressure. The level of the pressure was kept constant for all samples.

2.5. Handsheet Property Measurements. Tensile Strength. The TAPPI standard method of T494 om-96 was used to determine the tensile strength of paper. A sample length of 78 mm was used due to the size of the handsheet former as compared to the standard at 100 mm. A COM-TEN Universal Tester was used for testing samples. To validate our results with the COM-TEN Universal tester compared to the L&W Tensile Tester, tensile tests were carried out on both instruments using two different industrial copy paper samples. The tensile strength and the standard error of the mean for both samples are shown in the Supporting Information Table S1. The differences between the two sets of results were low (about 2.5 MPa), and therefore the COM-TEN tester was used confidently for tensile measurement of the handsheets.

Cobb Test. The water absorption to the paper was measured according to the TAPPI standard of T441 om-04. The samples were put in contact with water for 60 s, and the weight of the samples was measured by analytical balance before and after the test.

Detailed information on methods and materials is found in Miravkili.²³

3. RESULTS AND DISCUSSION

3.1. “Bounced Off” and “Sticky” Water Droplet: Roughness Effect. Two important properties are required for the fabrication of superhydrophobic surfaces, namely, surface roughness and low surface energy. Some microscale roughness on the surface of paper due to the shape and position of fibers and fines in the network does exist. However,

for superhydrophobic surfaces dual-scale roughness, micro- and nanoscale, is an important factor as well.

Plasma treatment on handsheets was performed in two steps. First, the samples were etched using O₂ plasma which is believed to create the nanoscale roughness on the paper. Then, the CF₄ was deposited on the surface of the handsheet to provide the low surface energy required. Vaswani⁸ reported that the O₂ plasma treatment oxidizes the surface due to hydroperoxide formation as well as reduces the surface by creation of carbon–oxygen double bonds in cellulose. However, the plasma processing conditions that are reported in these studies were aggressive since their focus was on the interfiber bonding, internal structure of fibers, and the coating distribution within the paper.¹⁶ In this work, the O₂ etching plasma was applied to alter the top layers of the handsheets and maintain the bulk properties.

Table 3 shows the water contact angle results for handsheets filled with PCC and clay fillers. These handsheets were

Table 3. Advancing Contact Angle Results before and after Plasma Treatment

paper	advancing contact angles (deg)			
	untreated	oxygen etched	CF ₄ deposited	O ₂ etched and CF ₄ deposited
fiber only	<5°	<5°	145° \pm 3	162° \pm 2
PCC	<5°	<5°	146° \pm 6	152° \pm 4
clay	<5°	<5°	144° \pm 7	160° \pm 6

prepared without any other chemical additives, i.e., containing only filler (25% loading) and fiber. Untreated samples and samples after O₂ etching were all hydrophilic, and the measurement of a stable static contact angle was impossible due to the quick absorption of water by the handsheets. The water droplet contact angle before complete absorption of water was measured and found to be approximately <5°. To understand the effect of etching on hydrophobicity, some of the handsheets were treated only by plasma CF₄ deposition on the surface without prior O₂ etching. The results show an increase in contact angle for the handsheets that were first etched and then were subjected to CF₄ deposition.

The XPS survey scan spectra of untreated and plasma-treated handsheets are shown in the Supporting Information Figure S2. The spectrum of the untreated handsheet mainly shows the presence of oxygen (O_{1s}) and carbon (C_{1s}) with the ratio of about 0.4 (C: 70.5% and O: 27.6%). The diagram also confirms the presence of a fluorine (F_{1s}) peak on both 15 and 20 min O₂ etched and CF₄-deposited handsheets. The XPS deconvoluted carbon spectra (C_{1s}) of untreated and plasma-treated handsheets were obtained using a curve-fitting program (Figure 1).

For the fittings the peak positions were fixed according to well-characterized binding energy shifts.¹⁸ According to Sahin¹⁸ cellulosic paper has a trimodal component C_{1s} XPS spectra peak pattern that is C–C, C–OH, and O–C–O at 285, 286.7, and 288 eV, respectively. These peaks are presented as C1, C2, and C3 in Figure 1. The spectrum of Figure 1(b) shows the presence of fluorine base functionalities on the handsheet surface at 289, 290.7, 294.8, and 293.1 eV (C4–C7). By considering the 0.25 eV error margin, these peaks can be assigned to CF₃–*CO–O, CF₂–CH₂, CF₃–CF₂*–O, and CF₂–*CF₂–O, respectively.¹⁸

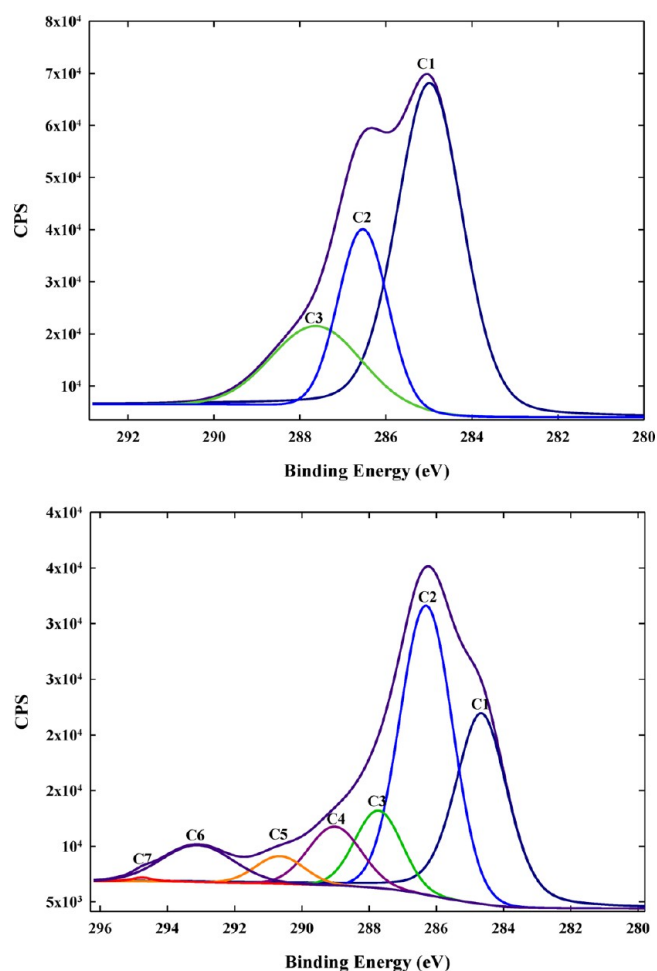


Figure 1. C_{1s} XPS spectra of (a) untreated handsheet and (b) 20 min O₂-etched and CF₄-deposited handsheet.

According to FTIR-ATR spectra for untreated and plasma-treated PCC-filled handsheets, the O₂ etching and CF₄ deposition result in suppression of cellulose absorption bands at 3334, 2906, and 1058 cm⁻¹. These wave numbers are

associated with O–H stretch, C–H stretch, and C–C–O stretch, respectively, which show a reduced level of oxygen and hydrogen on the surface (Figure S3, Supporting Information).¹¹

To demonstrate the effect of etching on the hydrophobicity of the handsheets, the dynamic effect of a free falling water droplet on the surface of handsheets was observed (Figure 2a–c). When the free falling water droplet was dispensed on the surface, it deformed heavily and bounced off completely from the surface of handsheets that were subjected to O₂ etching plus plasma CF₄ deposition (Figure 2c). However, on the handsheet that was treated only by CF₄ deposition, a small portion of the droplet pinned to the surface and prevented the droplet from completely bouncing off from the surface (Figure 2b). Figure 2d shows a rolling droplet on an inclined plasma-treated handsheet.

Figure 3a and 3b show the SEM results for samples before and after plasma treatment. As seen, the effect of O₂ etching on the surface of the handsheet is obvious in comparison with the handsheets that were only treated with CF₄. The surfaces of untreated handsheets and CF₄ deposited ones have some microscale roughness. The etching resulted in nanoscale roughness on the fiber surface and is accompanied by an increase in hydrophobicity. Figure 3c shows the effect of O₂ etching on a single fiber surface at higher magnification.

To confirm the effect of roughness on hydrophobicity, O₂ etching was performed for 15 and 20 min on the surface followed by CF₄ deposition. Figure 4 shows how contact angle changes for handsheet samples prepared at the two levels of etching time, 15 and 20 min, and with different filler levels. As seen the contact angles for handsheets that were subjected to 20 min etching are higher.

The fiber network provides the microscale roughness. However, it lacks the nanoscale roughness. Each cellulose fiber consists of microfibril bundles with the diameter ranging from 3 to 30 nm which can provide the nanoscale roughness that is required for superhydrophobicity.⁵ The microfibrils contain the crystalline cellulose moieties, and the matrix around the microfibrils is naturally amorphous.⁵ The O₂ plasma etched the surface of cellulose to a point that the microfibrils will be

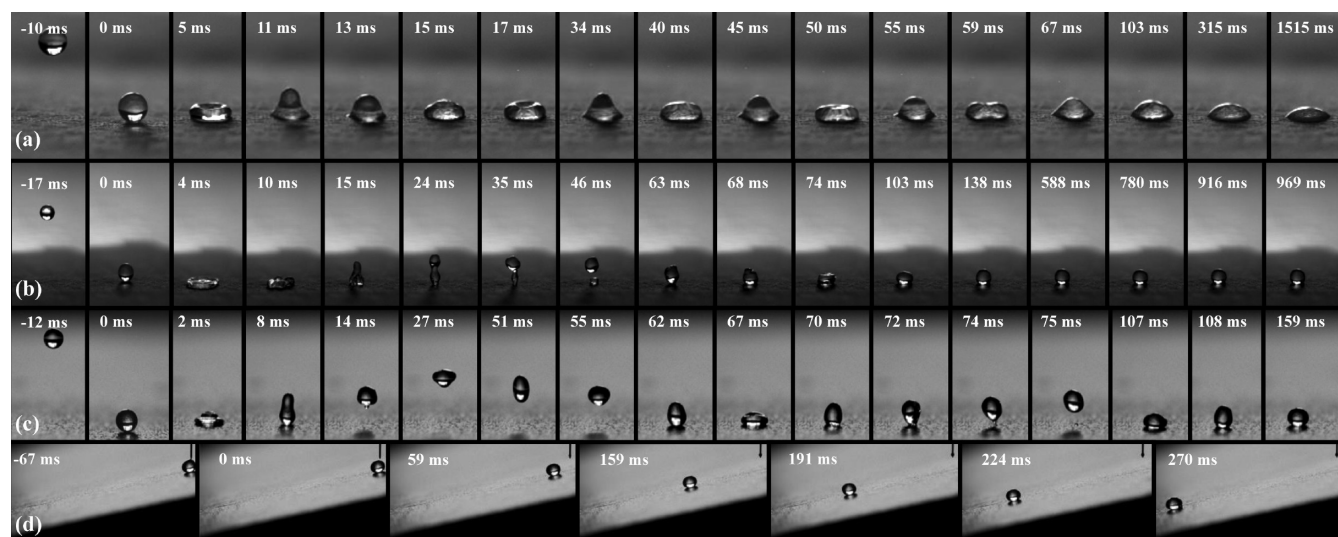


Figure 2. Images of (a) water droplet on the untreated handsheet, (b) sticky droplet on the CF₄-deposited handsheet, (c) bouncing off droplet on the O₂-etched and CF₄-deposited handsheet, and (d) a rolling droplet on the inclined handsheet surface (O₂ etched + CF₄ deposited).

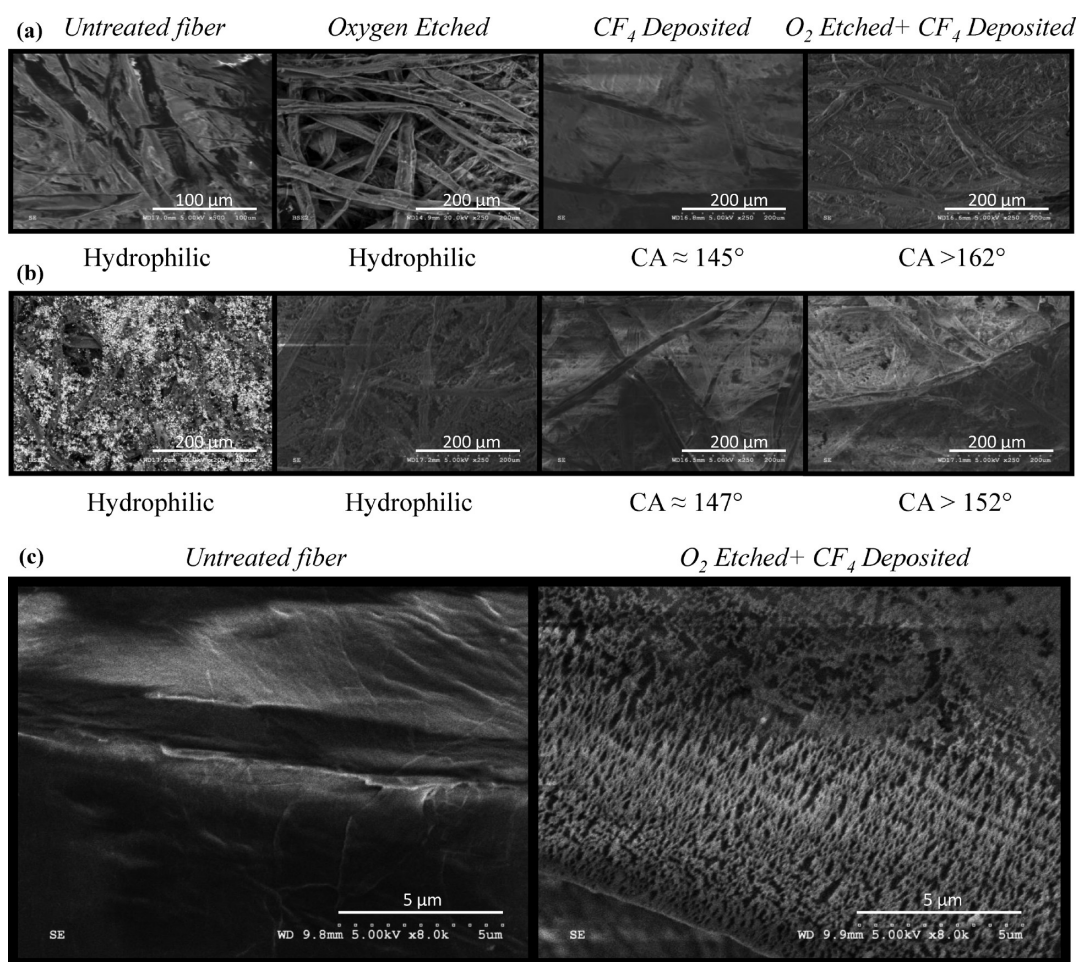


Figure 3. SEM micrographs (a) of handsheets without fillers, (b) of handsheets containing PCC fillers, and (c) at high magnification on a single fiber before and after plasma treatment.

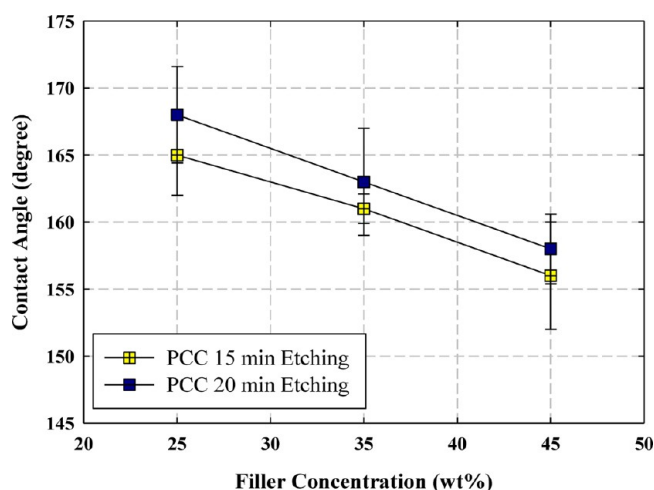
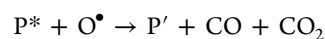
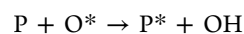


Figure 4. Effect of plasma etching time on hydrophobicity (O_2 etching and CF_4 deposition) of filled paper.

exposed and therefore the roughness will be created.^{5,11} It is believed that the amorphous regions of cellulose fiber are more susceptible to changes due to the low level of order in these regions.⁵ Also, most of the reactants penetrate the amorphous regions of cellulose and leave the intracrystalline regions unaffected.²⁴ Balu⁵ reported that in the etching process the O_2 species (O and O^*) will react with cellulose (P) and form OH ,

CO , and CO_2 and remove material from the surface according to the following reaction



Fiber Size Effect. The influence of adding classified fibers to unclassified fibers and fillers was evaluated. The contact angle results on the felt side of the handsheets are given in Table 4.

Table 4. Advancing Contact Angles on Handsheets Prepared with Classified and Unclassified Fibers after Plasma Treatment

tylor series no.	mean fiber length (mm)	advancing contact angle on felt side
48	1.5	$129^\circ \pm 2^\circ$
100	0.70	$131^\circ \pm 4^\circ$
200	0.36	$153^\circ \pm 3^\circ$

As seen from Table 4 the contact angle increases as the fiber length decreases. The difference in contact angle between the handsheets with fiber lengths of 1.5 and 0.7 mm is relatively low. However, the contact angle is significantly higher on a handsheet with fines (200 mesh, fiber length of 0.36 mm). It is believed²⁵ that the properties of fines are different than fibers due to fines small size (length) and larger surface area. It is also

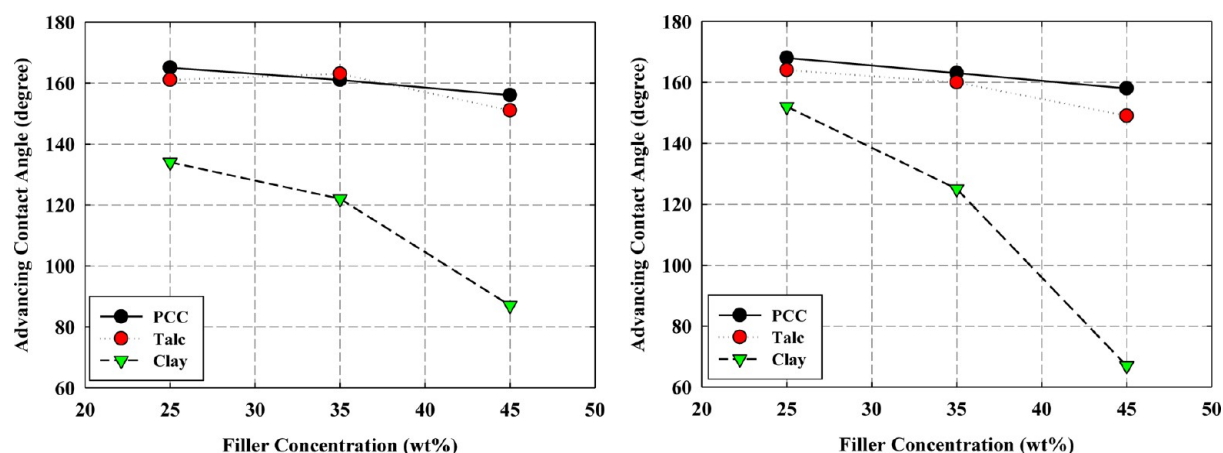


Figure 5. Felt side advancing contact angle of handsheets after plasma treatment at (CF_4 flow rate of $40 \text{ cm}^3/\text{min}$) (a) 15 min O_2 etching and (b) 20 min O_2 etching.

known that the amount of extractives and lignin is higher in the fines fraction, and this could explain the higher contact angle of handsheets prepared with the addition of fines.²⁶ Moreover, handsheets made with fines possess more hair-like roughness than those handsheets made with longer fibers.

3.2. Plasma Processing on Filled Handsheet, Filler Type, and Concentration Effect. The handsheet samples made with different fillers were subjected to O_2 etching followed by CF_4 deposition on the surface. All the plasma treatments were performed on the felt side of the handsheets. The dynamic contact angle was measured on both sides of the treated handsheets (felt side and wire side). Figure 5a and 5b shows the felt side advancing contact angle results for all treated handsheets (the errors associated with advancing contact angles are within $\pm 2^\circ$ to $\pm 4^\circ$ for all samples).

Before the treatment, the contact angles of all handsheets were found to be about 10° . As the results in Figure 5 show, the contact angle of all samples increased significantly after plasma treatment. However, the results show the contact angle decreases as filler concentration increases and is consistent for all three filler types. It can be concluded that the effect of plasma treatment on fiber is dominant as the amount of fiber decreases (or the concentration of filler increases). However, different fillers behave differently in terms of wettability. Some of the handsheets with clay fillers are still hydrophilic after the treatment. The different wetting behavior of the handsheets can be attributed to the different surface energies of the fillers. The reported surface energies for PCC, talc, and kaolin clay are 75–80, 35–40, and 550–600 J/cm^2 , respectively.²⁷ Therefore, the reason for lower contact angles of clay-filled handsheets is the highly polar surface of kaolin as well as its high surface energy.²⁸

By considering the surface energies, the handsheets filled with talc should result in higher contact angles than the handsheets filled with PCC. However, the PCC-filled handsheets were found to have the highest contact angles (Figure 5). This can be due to the different z -direction filler distribution on the handsheet. To confirm our hypothesis, the distribution of fillers in the felt (top) side, wire side, and z -direction (thickness) of the handsheets was examined by using SEM/EDX analysis.

In Fordrinier papermaking machines, the water is removed from one side of the sheet. This mechanism causes significant differences on the composition and microstructure of both sides of the sheet, referred to as “two sidedness” of paper.¹⁸

Figure 6 shows the amount of filler on the felt side, on the wire side, and in z -direction by determining the percent of a key element (Ca and Si). As seen there is no significant difference in distribution of filler for handsheets filled with talc and clay compared to the handsheets filled with PCC. For handsheets filled with PCC the calcium concentration on the wire side is higher than the felt side. This reveals the different behavior of PCC-filled handsheets. Since the PCC-filled handsheets have less filler on the felt side and the effect of plasma on fiber is dominant, the contact angle of the PCC-filled handsheets is higher than those filled with talc and clay. The handsheets with talc and clay have similar filler concentrations along the z -direction, whereas the calcium content of the handsheets filled with PCC has a different distribution with more Ca on the wire side.

3.3. Effect of CF_4 Flow Rate on Hydrophobicity. The effect of CF_4 flow rate during plasma treatment on the wetting behavior of the handsheets was examined. Prior to CF_4 deposition all the handsheets were subjected to O_2 etching. Figure 7 shows the contact angle on the felt side and wire side of PCC-filled handsheets at different CF_4 flow rates. Although the treatment was performed on the felt side of the handsheets, the wire side was also found to be hydrophobic. According to the results the hydrophobicity of the handsheets was shown to increase with CF_4 flow rate. It is mentioned in the literature that plasma treatment only affects the outermost surface.^{29,30} However, for porous materials the plasma treatment also treated the bulk material, and the depth of permeation can be controlled by plasma processing parameters.^{31,32} Therefore, the CF_4 flow rate was shown to be an influential plasma processing parameter.

3.4. Advancing and Receding (Dynamic) Contact Angles. The contact angle hysteresis was obtained by measuring the advancing and receding contact angles. After settling the water droplet gently on the surface, by growing and then shrinking the volume of the water droplet on the surface the advancing and receding contact angle was obtained (Figure 8a).

For superhydrophobic handsheets, or the “bouncing off” superhydrophobicity, dispensing of a water droplet on the surface was difficult, and the droplet was not detached from the pipet tip (Figure 8a). As the volume of the droplet increases, the three-phase contact line as well as the contact diameter suddenly extend. This sudden increase is associated with

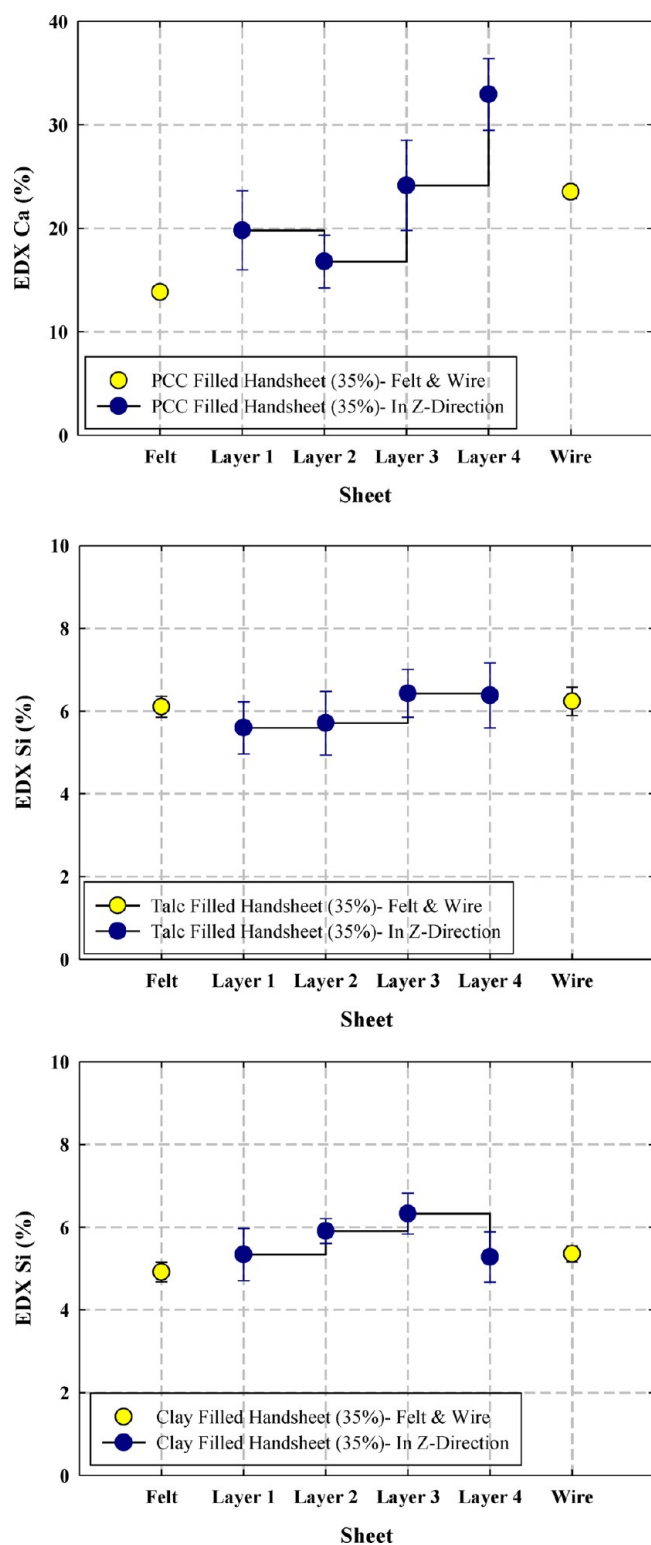


Figure 6. Filler distribution on the top side, wire side, and z-direction of handsheets with loading wt % of 35 (a) PCC, (b) talc, and (c) clay.

maximum contact angle or the advancing contact angle.³³ As the droplet shrinks, the receding contact angle is identified when it reaches a minimum, right before the contraction of the three-phase contact line. The purple image in Figure 8a is the advancing contact angle, and the pink image is the receding contact angle. The last image on the right shows that after growing and shrinking of the water droplet no water remained

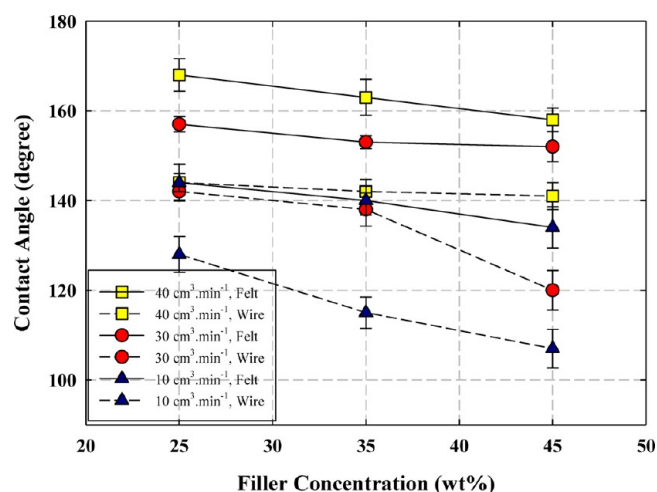


Figure 7. Comparison of advancing contact angles on the felt side and wire side for PCC-filled handsheets at 20 min O₂ etching and CF₄ deposition flow rate of 10, 20, and 40 cm³/min.

on the surface. Therefore, the surface is considered super-hydrophobic, and the droplet has no affinity for it. Also, the water droplet does not detach from the pipet tip and is lifted with it.

Figure 8b shows the advancing and receding contact angle values for the handsheets filled with 25 wt % PCC. The values of the advancing and receding contact angles of handsheets that were subjected to 15 and 20 min oxygen plasma followed by CF₄ deposition (40 cm³/min) are shown Table 5. The errors associated with advancing and receding contact angles are within $\pm 2^\circ$ to $\pm 4^\circ$ for all samples.

3.5. Handsheet Properties Tests and Tensile and Cobb Values. *Tensile Strength.* The tensile strength of all handsheets was measured, and the results are shown in Figure 9 for CF₄-treated PCC-filled handsheets (see Supporting Information Figure S4 for clay-filled and talc-filled handsheets). It was shown that as the filler content in paper increases the tensile strength of paper decreases. It was also seen that the plasma treatment causes a decrease in the tensile strength of handsheets. As the oxygen etching time increases the tensile strength decreases. This is due to the reduction of mechanical properties in the thin surface layer of handsheets. Sahin et al.²⁹ reported that the cellulose bonds, at “intra- and interfiber crossings”, were influenced by plasma treatment.

By comparing the effect of filler type on tensile strength of handsheets (Figure 10), at low concentration of filler (25%) the PCC-filled handsheets have higher tensile strength. However, as the concentration of filler (clay and talc) increases (35% and 45%), it results in higher tensile strength compared to PCC-filled handsheets at the same concentration. It has been reported³⁴ that the plate-like structure of kaolin clay and talc has a less negative effect on fiber–fiber bonding, and they can be used at higher concentrations. Thus, the shape of the filler particle has an impact on the tensile strength of the handsheet.

Cobb Values. The Cobb values were obtained for the water absorption capacity of the handsheet, and the results are given in Table 6. The Cobb values are in agreement with the contact angle results as PCC-filled handsheets have the lowest water absorption, while the clay-filled handsheets have the highest water absorption. Also, as the etching time increases the Cobb values decrease.

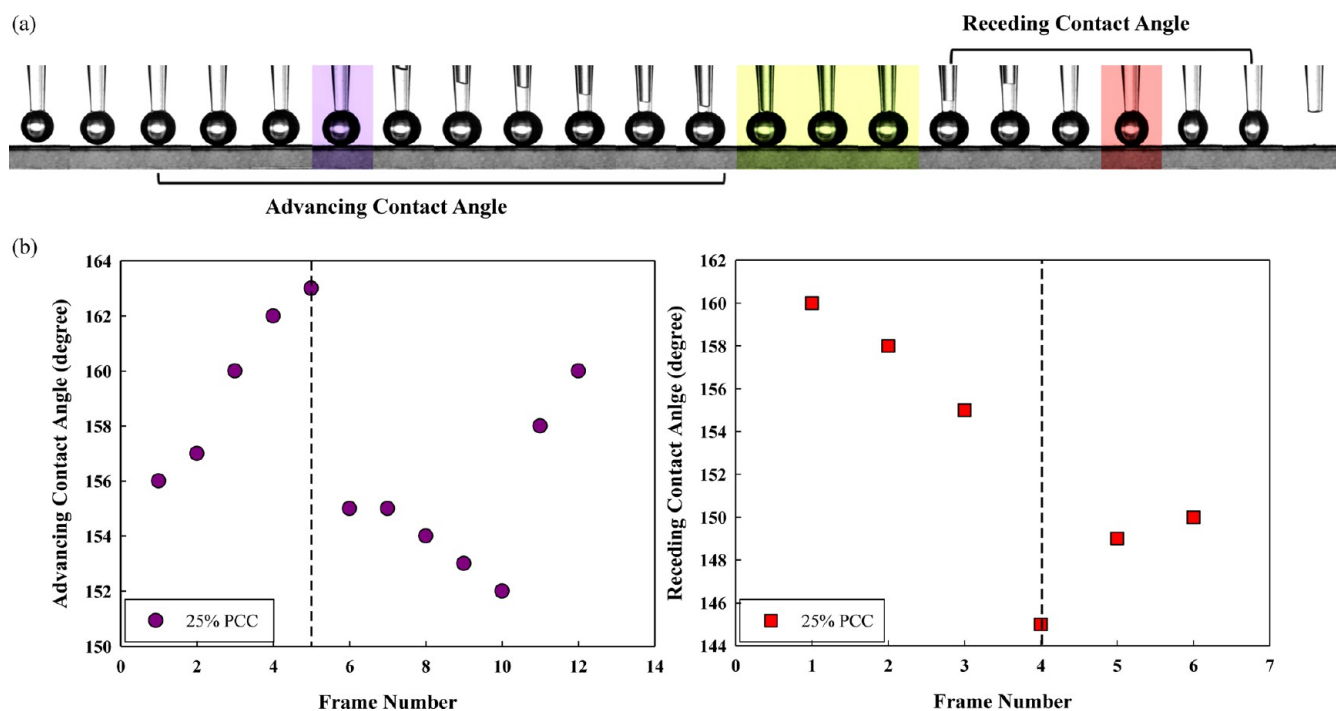


Figure 8. Advancing and receding (a) water droplet on the superhydrophobic PCC-filled handsheet and (b) contact angles for the PCC-filled handsheet.

Table 5. Dynamic (Advancing and Receding) CAs on Handsheets

		O ₂ 20 min, CF ₄ 40 cm ³ /min								
		PCC			talc			clay		
sheet side	filler concentration (wt %)	θ_{adv}	θ_{rec}	<i>H</i>	θ_{adv}	θ_{rec}	<i>H</i>	θ_{adv}	θ_{rec}	<i>H</i>
felt	25	168	158	10	164	154	10	152	131	21
	35	163	153	10	160	150	10	125	99	26
	45	158	152	6	149	143	6	67	55	12
wire	25	144	135	9	165	158	7	161	151	10
	35	142	130	12	162	156	6	154	142	12
	45	141	129	12	161	154	7	94	74	20
		O ₂ 15 min, CF ₄ 40 cm ³ /min								
		PCC			talc			clay		
sheet side	filler concentration (wt %)	θ_{adv}	θ_{rec}	<i>H</i>	θ_{adv}	θ_{rec}	<i>H</i>	θ_{adv}	θ_{rec}	<i>H</i>
felt	25	165	157	8	161	148	13	134	114	20
	35	161	153	8	163	149	14	122	95	27
	45	156	149	7	151	139	12	87	75	12
wire	25	166	159	7	162	155	7	164	154	10
	35	156	144	12	155	148	7	132	110	22
	45	141	120	21	150	133	17	118	80	38

The Cobb values show minor absorption of water in the handsheet. This may raise the question if there is absorption of water droplets on the surface of handsheets during contact angle measurements. After analyzing the contact angles it was found that there was no significant change in the contact angle values, which demonstrates that there is no detectable absorption of water in the handsheet (Table 7).

Although the handsheets were hydro- and superhydrophobic, their water vapor transmission rates were in the order of 300–400 g m⁻² day⁻¹, and thus they were not a good water vapor barrier (further discussion in Supporting Information Figure S5). Thus, the samples prepared in this work have properties desired for applications where breathable but water-repellent paper is required.

4. CONCLUSIONS

In this work it was shown that dual-scale roughness is a key property for the fabrication of superhydrophobic paper from lignocellulosic wood fibers and mineral fillers. The process of O₂ plasma etching followed by fluorocarbon deposition resulted in superhydrophobic paper with low hysteresis. However, paper only treated by fluorocarbon plasma resulted in a “sticky” hydrophobic (high hysteresis) surface. The contact angle of paper samples made with different fiber length was found to increase as the fiber length decreases. Another important factor was the effect of mineral filler type and concentration on the wettability of paper samples. After the plasma treatment, although the contact angles on all of the paper samples filled

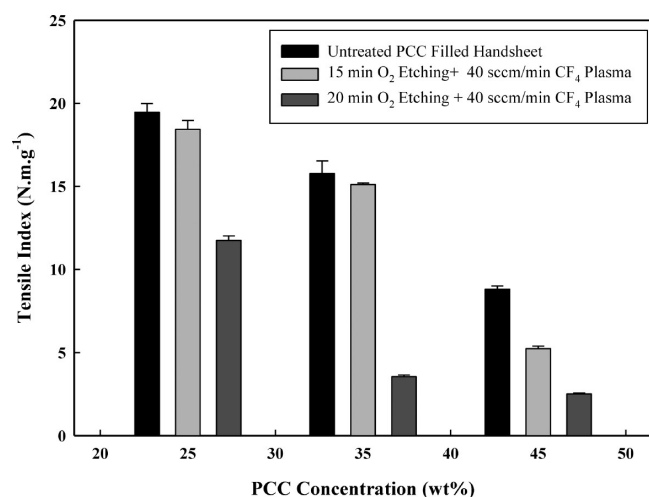


Figure 9. Tensile index of PCC-filled handsheets before and after plasma treatments.

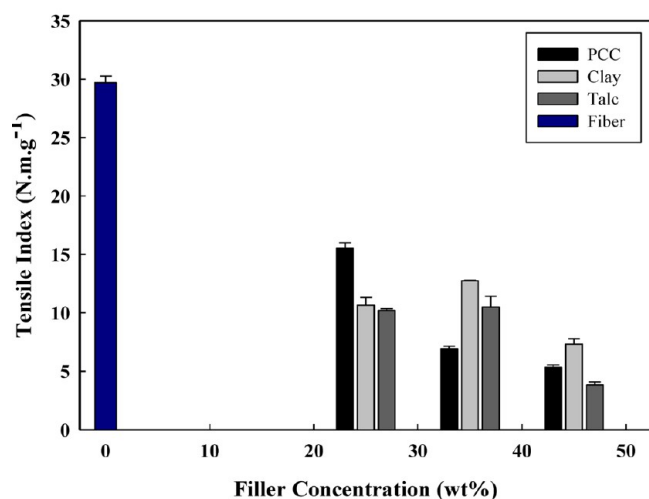
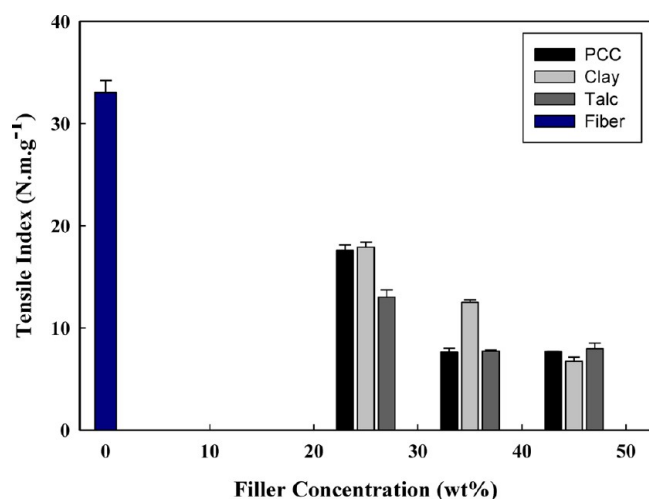


Figure 10. Effect of filler type on the tensile strength after plasma treatment with 30 cm³/min CF₄ and O₂ etching of (a) 15 min and (b) 20 min.

with calcium carbonate, talc, and clay increase, the paper samples filled with kaolin clay remained hydrophilic for high concentrations of filler (45%). Furthermore, it was shown that plasma processing has a negative effect on tensile strength of

Table 6. Cobb Values for Handsheets after Plasma Treatment

sample	Cobb value (g/m ²)	
	15 min O ₂ Etching + CF ₄	20 min O ₂ etching + CF ₄
PCC	25%	5.40
	35%	5.40
	45%	5.40
talc	25%	5.40
	35%	7.20
	45%	9.00
clay	25%	7.20
	35%	14.40
	45%	26.99

Table 7. Contact Angles of Droplets over 1 min

time (s)	contact angles (deg)			
	PCC (35%)	clay (35%)	talc (35%)	fiber only
0	141	141	142	145
10	141	142	143	144
20	140	143	142	144
30	141	140	142	146
40	141	141	143	145
50	141	143	142	146
60	142	142	143	145

handsheets. Comparing the tensile index values, it is seen that as the etching time increases the tensile strength of handsheets decreases. It is recognized that the plasma processing time in this laboratory study is high for industrial applications. However, it can be noted that the plasma treatment processing is currently used in the textile industry. For an industrial application of the methods presented in this work a higher plasma power would be required to shorten the processing time.

ASSOCIATED CONTENT

Supporting Information

Detailed sampling procedure for SEM/EDX analysis, tensile strength results for L&W Tensile Tester vs COM-TEN tester, XPS and FTIR survey spectra, tensile index values, and water vapor transmission rate results. This material is available free of charge via the Internet at <http://pubs.acs.org>.

AUTHOR INFORMATION

Corresponding Author

*E-mail: peter.englezos@ubc.ca.

Notes

The authors declare no competing financial interest.

ACKNOWLEDGMENTS

The financial support from the Wood Fiber Network and NSERC is appreciated. Thanks to Madjid Farmahini Farahani for doing the WVTR tests at university of New Brunswick. Thanks to Reza Korehei for FTIR analysis.

REFERENCES

- (1) Yan, Y. Y.; Gao, N.; Barthlott, W. *Adv. Colloid Interface Sci.* **2011**, *169*, 80–105.
- (2) Liu, K.; Tian, Y.; Jiang, L. *Prog. Mater. Sci.* **2013**, *58*, 503–564.
- (3) Groenendijk, M. *Laser Tech. J.* **2008**, *5*, 44–48.

- (4) Goncalves, G.; Marques, P. A. A. P.; Trinadade, T.; Neto, C. P.; Gandini, A. J. *Colloid Interface Sci.* **2008**, *324*, 42–46.
- (5) Balu, B.; Breedveld, V.; Hess, D. W. *Langmuir* **2008**, *24*, 4785–4790.
- (6) Shen, J.; Qian, X. *BioResources* **2012**, *7*, 4495–4498.
- (7) Hubbe, M. A. *BioResources* **2006**, *2*, 106–145.
- (8) Vaswani, S.; Koskinen, J.; Hess, D. W. *Surf. Coat. Technol.* **2005**, *195*, 121–129.
- (9) Balu, B.; Kim, J. S.; Breedveld, V.; Hess, D. W. *Contact Angle, Wettability Adhes.* **2009**, *6*, 235–249.
- (10) Balu, B.; Kim, J. S.; Breedveld, V.; Hess, D. W. *J. Adhes. Sci. Technol.* **2009**, *23*, 361–380.
- (11) Balu, B. Plasma Processing of Cellulose Surfaces and Their Interactions with Fluids. *Ph.D. Thesis*, Georgia Institute of Technology, USA, December 2009.
- (12) Wertheim, M.; Suranyi, G.; Goring, D. A. I. *Tappi* **1972**, *55*, 1707.
- (13) Pykonen, M.; Johansson, K.; Dubreuil, M.; Vangeneugden, D.; Strom, G.; Fardim, P.; Toivakka, M. *J. Adhes. Sci. Technol.* **2010**, *24*, 511–537.
- (14) Carlsson, C. M. G.; Strom, G. *Langmuir* **1991**, *7*, 2492–2497.
- (15) Strom, G.; Carlsson, C. M. G. *J. Adhes. Sci. Technol.* **1992**, *6*, 745–761.
- (16) Sapieha, S.; Wrobel, A. M.; Wertheimer, M. R. *Plasma Chem. Plasma Process.* **1988**, *8*, 331–346.
- (17) Sapieha, S.; Verreault, M.; Klemberg-Sapieha, J. E.; Sacher, E.; Wertheimer, M. R. *Appl. Surf. Sci.* **1990**, *44*, 165–169.
- (18) Sahin, H. T. *Appl. Surf. Sci.* **2007**, *253*, 4367–4373.
- (19) Montgomery, J. The Role of Suction Boxes on Forming Section Retention and Filler Migration. *M.A.Sc. Thesis*, University of British Columbia, Vancouver, B.C., August 2010.
- (20) Motiee, S. Effect of Chemical Additives on Z-Direction Filler Distribution in Paper. *M.A.Sc. Thesis*, University of British Columbia, Vancouver, B.C., April 2013.
- (21) Sang, Y.; McQuaid, M.; Englezos, P. *BioResources* **2011**, *6*, 656–671.
- (22) Stamboulidis, C.; Englezos, P.; Hatzikiriakos, S. G. *Tribol. Int.* **2013**, *57*, 177–183.
- (23) Mirvakili, M. Superhydrophobic Fiber Networks Loaded with Functionalized Fillers. *M.A.Sc. Thesis*, University of British Columbia, Vancouver, B.C., January 2013.
- (24) Ciolacu, D.; Ciolacu, F.; Popa, V. I. *Cell. Chem. Technol.* **2011**, *45*, 13–21.
- (25) Vaino, A. K.; Paulapuro, H. *BioResources* **2007**, *2*, 442–458.
- (26) Vander Wielen, L. C. Dielectric Barrier Discharge-Initiated Fiber Modification. *Ph.D. Thesis*, Georgia Institute of Technology, USA, June 2004.
- (27) Sharma, S.; Bash, W. *TAPPI Coat. Conf., Proc.* Atlanta, GA, 1998.
- (28) Salmah, H.; Ruzaidi, C. M.; Supri, A. G. *J. Phys. Sci.* **2009**, *20*, 99–107.
- (29) Sahin, H. T.; Manolache, S.; Young, R. A.; Denes, F. *Cellulose* **2002**, *9*, 171–181.
- (30) Navarro, F.; Davalos, F.; Denes, F.; Cruz, L. E.; Young, R. A.; Ramos, J. *Cellulose* **2003**, *10*, 411–424.
- (31) Mukhopadhyay, S. M.; Joshi, P.; Datta, S.; Macdaniel. *Appl. Surf. Sci.* **2002**, *201*, 219–226.
- (32) Tu, X.; Young, R. A.; Denes, F. *Cellulose* **1994**, *1*, 87–106.
- (33) Yeh, K. Y.; Chen, L. J. *Langmuir* **2008**, *24*, 245–251.
- (34) Effect of Fillers on LWC. *IMERYS Paper & Packaging Technical Guides*; Imerys: Paris, Nov. 2008.